

Origin of W UMa-type contact binaries - age and orbital evolution

M. Yıldız*

Department of Astronomy and Space Sciences, Ege University, Bornova, 35100 İzmir, Turkey

Accepted 2005 December 15. Received 2005 December 14; in original form 2005 October 11

ABSTRACT

Recently, our understanding of the origin of W UMa-type contact binaries has become clearer. Initial masses of their components were successfully estimated by Yıldız and Doğan using a new method mainly based on observational properties of overluminous secondary components. In this paper, we continue to discuss the results and make computations for age and orbital evolution of these binaries. It is shown that the secondary mass, according to its luminosity, also successfully predicts the observed radius. While the current mass of the primary component is determined by initial masses, the current secondary mass is also a function of initial angular momentum. We develop methods to compute the age of A- and W-subtype W UMa-type contact binaries in terms of initial masses and mass according to the luminosity of the secondaries. Comparisons of our results with the mean ages from kinematic properties of these binaries and data pertaining to contact binaries in open and globular clusters, have increased our confidence on this method. The mean ages of both A- and W-subtype contact binaries are found as 4.4 and 4.6 Gyr, respectively. From kinematic studies, these ages are given as 4.5 and 4.4 Gyr, respectively. We also compute orbital properties of A-subtype contact binaries at the time of the first overflow. Initial angular momentum of these binaries is computed by comparing them with the well-known detached binaries. The angular momentum loss rate derived in the present study for the detached phase is in very good agreement with the semi-empirical rates available in the literature. In addition to the limitations on the initial masses of W UMa-type contact binaries, it is shown that the initial period of these binaries is less than about 4.45 d.

Key words: binaries: close - binaries: eclipsing - stars: evolution - stars: interior - stars: late-type.

1 INTRODUCTION

The stars themselves are mysterious enough to study. W UMa-type contact binaries (CBs) are, in many respects, excellent objects to research, being among the most observed stars and having experienced mass transfer between components. The observational data of individual systems and statistical properties of entire data show so many regular and irregular variations that many contradictory ideas concerning their structure and evolution have been perpetuated. Recently, Yıldız & Doğan (2013, hereafter Paper I) have discovered a new method to compute the initial masses of component stars from the observed masses and luminosity of the secondary component. This method gives the initial mass range for the secondaries as $M_{2i}=1.3\text{-}2.6 M_{\odot}$. That of the primaries is $M_{1i} = 0.2 - 1.5M_{\odot}$, which is in very good agreement with the required mass range for the angular momentum loss process via magnetic braking (Tutukov, Dremova & Svechnikov 2004). Moreover, the initial masses of A- and W-subtypes have completely different ranges for their secondaries: $M_{2i} > 1.8M_{\odot}$ for the former and $M_{2i} < 1.8M_{\odot}$ for the latter. In the present study, we further

discuss some results of Paper I and develop new methods for estimation of age and angular momentum loss rates in detached and CB phases.

The formation history of A-subtype CBs is controlled in the pre-contact phase by two effects, namely, nuclear evolution of the massive component ($M_{2i}=1.8\text{-}2.7 M_{\odot}$) and angular momentum evolution of the lighter component ($M_{1i}=0.2\text{-}1.5 M_{\odot}$). Depending on the initial masses and angular momentum reservoir, the detached phase ends up near the terminal-age of the main-sequence (TAMS) line in the Hertzsprung–Russel diagram (HRD). In the precursors of W-subtype CBs, however, both components experience efficient angular momentum loss throughout or during part of their main-sequence MS phase of the massive component. For some of their progenitors, angular momentum evolution is so fast that the components may come into contact with each other before the massive component becomes a TAMS star. The maximum mass of their massive components is $1.8 \pm 0.1 M_{\odot}$. In addition, for stars with $1.5 < M_{2i} < 1.8 M_{\odot}$ the secondary star is not effective in angular momentum loss process in the early detached phase of binary evolution, but becomes effective as its convective zone deepens during evolution towards the TAMS line in the HRD.

For a typical A-subtype CB, the total initial mass is $\overline{M_{T1}} =$

* E-mail: mutlu.yildiz@ege.edu.tr

$\overline{M}_{1i} + \overline{M}_{2i} = 3.0 M_{\odot}$. The mean initial masses of the secondary and primary components are $\overline{M}_{2i} = 2.0$ and $\overline{M}_{1i} = 1.0 M_{\odot}$, respectively. The mean total initial mass of W-subtype, however, is $\overline{M}_{Ti} = 2.5$, $0.5 M_{\odot}$ less than that of A-subtype CBs. For W-subtype CBs, $\overline{M}_{2i} = 1.7 M_{\odot}$ and $\overline{M}_{1i} = 0.8 M_{\odot}$.

Age determination of W UMa-type CBs is very important for a better understanding of binary evolution. In addition to initial masses, if period (P) or orbital dimension is estimated at the time of the first overflow (FOF), for example, one can compute initial angular momentum and then deduce the rate of angular momentum loss as a first approximation. A similar computation can also be made for the mass-loss. The present study also aims to make such computations.

Binaries have a variety of periods. If one of the components is a late-type star in the detached phase, then angular momentum loss causes the orbital period to decrease. If both components are late-type, then angular momentum evolution is nearly twice as fast. This may be the reason why W UMa-type CBs are observed in relatively young open clusters, such as in Praesepe. Angular momentum evolution is one of the essential problems in stellar astrophysics and has been the subject of many papers on single or binary stars in the literature (van 't Veer 1991; Eggleton, 2001; Demircan et al. 2006; Stepień, 2006; Gazeas & Stepień 2008). Although magnetic braking and tidal locking in binaries with late-type components are very complicated processes, the angular momentum loss rates for such binaries derived by Stepień (2006, see also Gazeas & Stepień 2008) and Demircan et al. (2006) are very easy to apply. We compare our results on angular momentum evolution of the detached precursors of W UMa-type CBs with these rates (see Section 4.2).

The final end stage of evolution of W UMa-type CBs is also debated in the literature (see, e.g., Li et al. 2007; Eker, Demircan & Bilir 2008). The fate of a W UMa-type CB essentially depends on the ratio of angular momentum and mass-loss during the contact phase. These systems seem to be the progenitors of blue stragglers observed in many clusters. Some of the blue stragglers are single stars and it seems reasonable to suppose that these were formed by merging components of W UMa-type CBs. In this case, the rate of angular momentum loss is so high that the components merge. On the other hand, if mass-loss rate is very high, then the component stars remain separate. The final form will then consist of either two brown dwarfs (Li et al. 2007) or two stars with very low mass. In the latter case, the age of the stars becomes infinitely long. In order to predict the final products, further studies are required for mass and angular momentum loss rates in the W UMa-type CB phase.

The remainder of this paper is organized as follows. In Section 2, some basic results of Paper I are summarized and the $M_L - R$ relation for W UMa-type CBs is compared with that of the well-known detached eclipsing binaries (DEBs). Section 3 is devoted to the method for age computation of A- and W-subtype CBs and a comparison of results with cluster member close binaries. Orbital parameters of CBs and their evolution are considered and discussed in Section 4. Finally, our concluding remarks are given in Section 5.

2 THE INITIAL MASSES OF W UMA-TYPE CBS AND CONNECTION WITH THEIR STRUCTURES

2.1 Mass according to luminosity and radius relation

The secondary components of the W UMa-type CBs are over-luminous and over-sized according to their masses. In Paper I,

Yıldız and Doğan consider this to be a result of the initial masses being much higher than the present (observed) masses. They define M_L of a secondary star as the mass according to its observed luminosity (L_2) by assuming $L_2 = L_{TAMS}$: $M_L = (L_2/1.5)^{0.237}$. They construct interior models with mass-loss by using the MESA stellar evolution code (Paxton et al. 2011) and find a relation between the mass differences $\Delta M = M_{2i} - M_2$ and $\delta M = M_L - M_2$, where M_2 is the present mass of the secondaries. The expression derived from these models for initial mass of the secondary components in Paper I is a function of the mass difference δM and M_2 : $M_{2i} = M_2 + 2.50(\delta M - 0.07)^{0.64}$, where the masses are in units of solar mass.

We want to test if M_L is successful in predicting the present radii. R_2 of A- and W-subtypes are plotted with respect to M_2 and M_L in Figs. 1(a) and (b). We use the same data set as in Paper I. The components of well-known DEBs are also shown for comparison (Southworth, DEBCat: <http://www.astro.keele.ac.uk/jkt/debcats/>). The secondary components are very large for their mass M_2 . Hilditch, King & McFarlane (1988) have found that the radii of secondaries of the W-subtype CBs are 1.5 times larger than normal. Although they have reported much larger factors for the secondaries of A-subtype CBs, we find that the difference between the radii of the secondaries and normal stars is simply $0.5 R_{\odot}$. For example, a normal star of $0.4 M_{\odot}$ has a radius of $0.4 R_{\odot}$ (CU Cnc), but the radius of a secondary component in an A-subtype CB of the same mass (AQ Psc) is $0.9 R_{\odot}$. For W-subtype, there is no such single relation but a decreasing difference as mass increases.

The relation between R_2 and M_L , however, is very close to the $M - R$ relation for the components of DEBs. This is a very good indicator for the fact that the entire structure of a secondary star with M_L is very close to that of a single star with mass $M_* = M_L$. This result is somewhat surprising because one may expect that the oversized behaviour of a secondary star is mainly determined by the presence of a close companion.

The slight differences between the $M_L - R$ relation for both A- and W-subtypes and the $M - R$ relation for DEBs are noticeable for low mass secondaries ($M_2 < 0.15 M_{\odot}$, $M_L = 0.5 - 0.8 M_{\odot}$). This is most likely due to the influence of a very close companion ($P < 0.38$ d and $a < 2.7 R_{\odot}$) on the secondary radius.

In the light of these results we assume that the secondaries' internal structure is similar to that of a star with the mass M_L . If these stars were isolated with their present features, then their MS lifetime would be given by M_L rather than M_2 . This point has strong significance for our method to compute the ages of W UMa-type CBs (see Section 3).

2.2 Correlation between initial and present masses

It is well known that the gravitational force between two masses depends on the product of their masses and the inverse square of the distance between them. We have the initial masses but not the distances between the component stars in their detached phase. Therefore, we consider the product of initial masses ($M_{1i} M_{2i}$) as a measure of tidal interaction. In Fig. 2(a) this product for A- and W-subtypes is plotted with respect to the primary present mass M_1 . The solid line is for the curve fitted to the data. The present mass of the primary components is strongly dependent on their initial masses. The other parameters – such as initial angular momentum, period and age of systems – have no role. In Fig. 2(b), the total initial mass is plotted against M_1 . There is a very clear linear relation between M_{Ti} and M_1 . The fitting line is found as

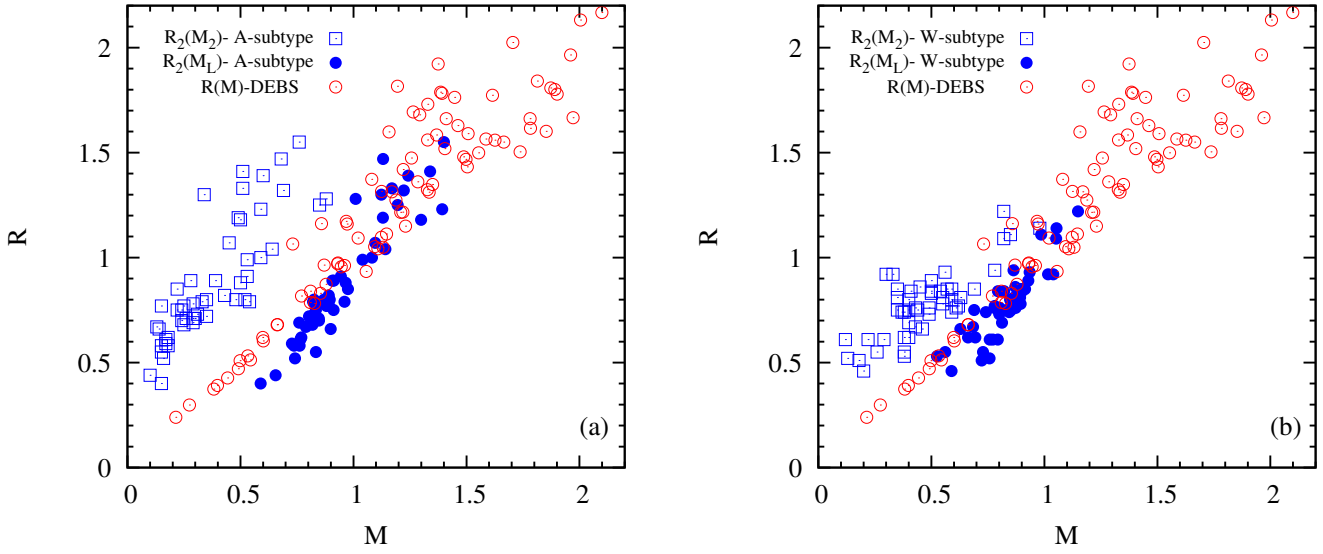


Figure 1. The mass–radius relation for secondaries of the A- (a) and W-subtype (b) CBs (square). The filled circles represent mass according to luminosity–radius relation. For comparison, the components of the well-known DEBs (circles) are also plotted. Solar units are used.

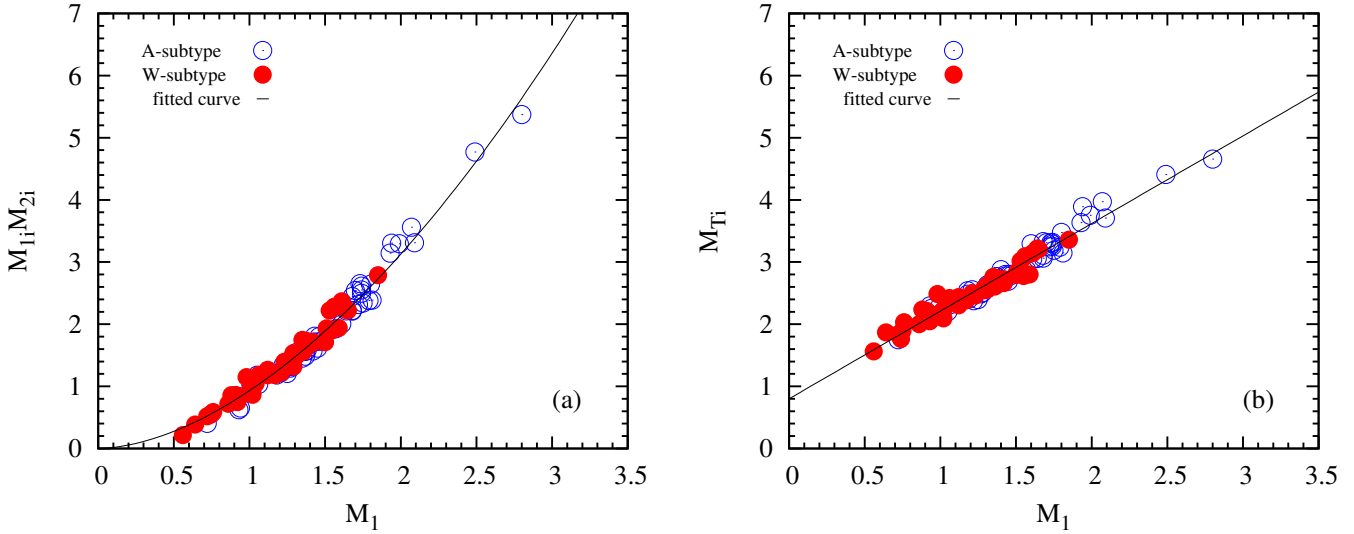


Figure 2. Product (a) and summation (b) of initial masses of component stars as a function of the present mass of the primary component. The fitted curve is $(0.93 \pm 0.01)(M_1/M_\odot)^{1.75 \pm 0.02}$ in (a) and $(1.41 \pm 0.03)M_1/M_\odot + (0.80 \pm 0.04)$ in (b).

$M_{T_1} = 1.41M_1 + 0.80$. M_1 can be computed from this equation as a function of initial masses (in solar mass):

$$M_1 = 0.71(M_{1i} + M_{2i}) - 0.57. \quad (1)$$

The maximum difference between the observed and computed M_1 from equation (1) is less than 10 per cent. This implies that the mass of the primary either remains constant or changes very little during the W UMA phase.

In Fig. 3, the total initial mass M_{T_1} is plotted against the present total mass $M_T = M_1 + M_2$. The relation between M_{T_1} and M_T is also linear. The mean difference between M_{T_1} and M_T is $1.05 M_\odot$ for A- and $0.82 M_\odot$ for W-subtype CBs. This shows that the A-subtype CBs have lost, on average, a mass $0.23 M_\odot$

higher than W-subtype CBs. The data are a bit more scattered in Fig. 3 than in Fig. 2(b). This implies that M_2 also depends on some other initial parameters as well as initial masses (see Section 4).

3 AGE OF W UMA-TYPE CBs

Age of a normal star can be found by some methods based on comparison of a computer model and observational parameters. Time variation of stellar parameters allows such methods. For a normal MS star with non-astroseismic constraints, the highest (and monotonic) changing (observable) parameters are luminosity and radius. However, these parameters are a very sensitive function of mass,

and composition. If uncertainty in mass is high, then an accurate age is difficult to obtain. If the uncertainty in mass is about 10 per cent, then age uncertainty is about 30 per cent. In comparison, the effect of metallicity on age is greater. For example, a $1.5 M_{\odot}$ model with solar composition ($X=0.7024$, $Z=0.0172$) has an MS lifetime of 2.1 Gyr. In comparison when $Z=0.0322$, the age for a star of the same mass is 3.2 Gyr, a 50 per cent longer MS lifetime. Therefore, any ages we find and estimate have some inherent uncertainty.

On the other hand, even in the cases where we fit interior models to asteroseismic constraints to find an age the agreement with other derived ages can be poor. For alpha Centauri A and B, for example, ages from the non-asteroseismic and asteroseismic constraints are found as about 9 Gyr and 5.6-5.9 Gyr (see, Miglio & Montalbán 2005; Yıldız 2007a), respectively. Therefore, even with the best state-of-the-art observational results there can still be some dispute or uncertainty about the age of a star, this is compounded in the case of binary stars where binary interactions will make it difficult to determine the true age. This is in addition to the effect of uncertain current/initial stellar composition. Below, we therefore aim to develop a method for determination of the age of observed W UMa binaries in terms of the variable of stellar mass only to yield a rough, but useful, stellar age.

As stated by Hilditch, King & McFarlane (1988), the secondaries of A-subtype CBs are more evolved than that of W-subtype CBs. Then, we anticipate that the detached phases of precursors of A- and W-subtype CBs are quite different. The secondary stars at the end of this phase may overflow their Roche lobe for two very different reasons:

- (i) due to rapid expansion after TAMS or
- (ii) due to the Roche lobe receding as a result of rapid orbital (angular momentum) evolution.

In case (i), the detached phase lasts about t_{MS} of the secondary star. This is simply the formation course of A-subtype. Since $M_{2i} > 1.8M_{\odot}$ for A-subtype, the duration of the detached phase (t_{D}) is less than $t_{\text{MS}}(1.8M_{\odot})$. In case (ii), angular momentum loss rate is high because both components are effective in the detached phase. This occurs in the precursors of W-subtype CBs. Their detached phase is shorter than the MS lifetime of their secondaries, $t_{\text{D}} \ll t_{\text{MS}}(M_{2i})$. The shortest value of t_{D} for W-subtype with $M_{2i} < 1.8M_{\odot}$ is $t_{\text{MS}}(1.8M_{\odot})/2$ (see below).

3.1 Age of A-subtype CBs

If M_{2i} is higher than $1.8 M_{\odot}$, then only the primary component is effective in the angular momentum loss process via magnetic braking. Such binaries become A-subtype. Since their angular momentum evolution is relatively slow, the Roche lobe overflow merely starts (i.e. mass transfer) after the secondary component completes its MS lifetime.

The mass transfer process obscures stellar quantities such as age. Therefore, it seems to be very difficult to assign age to the W UMa-type CBs as they have three different evolutionary phases - namely, detached, semidetached (SD) and CB phases. Current age of a CB system (t) is the summation of durations of three phases. They are detached (t_{D}), SD (t_{SD}) and contact phases (t_{CB}). Then,

$$t = t_{\text{D}} + t_{\text{SD}} + t_{\text{CB}}, \quad (2)$$

where t_{CB} is the time from the beginning of contact phase until present. As stated above, for A-subtype CBs, the time interval for the detached phase is very nearly the same as the MS lifetime of the

Table 1. Mean ages of A- and W-subtype CBs. The ages taken from Bilir et al. (2005) are the mean kinematical ages.

Type	Age (Gyr)	Age (Gyr)
A-subtype	4.37 ± 1.23	4.48
W-subtype	4.63 ± 1.48	4.37
	Present Study	Bilir et al. (2005)

secondary star: $t_{\text{D}} \approx t_{\text{MS}}(M_{2i})$. One can precisely compute t_{MS} as a function of M_{2i} . Yıldız (2013) derives an expression for t_{MS} from stellar evolution models as

$$t_{\text{MS}} = \frac{10}{(M/M_{\odot})^{4.05}} (5.60 \cdot 10^{-3} (\frac{M}{M_{\odot}} + 3.993)^{3.16} + 0.042) \text{ Gyr}. \quad (3)$$

The detached phase of the precursor of an A-subtype system lasts slightly longer than the MS lifetime of its massive component [$t_{\text{MS}}(M_{2i})$]. This time interval is very short for systems with high initial mass. On the other hand, the age of a system with a secondary of mass M_L must be less than $t_{\text{MS}}(M_L)$, or, more generally, $t_{\text{MS}}(M_{2i}) < t < t_{\text{MS}}(M_L)$ (see below). From these constraints, we can derive an expression for $t_{\text{SD}} + t_{\text{CB}}$.

After the detached phase, nuclear and secular evolution develop under control of each other. The SD phase starts with M_{2i} and M_L is the present presumptive mass according to luminosity. The upper limit for these binaries, however, is the MS age of a star with a mass of $M = M_L$. The MS age of such an isolated star is $t_{\text{MS}}(M_L)$. In general, $t_{\text{MS}}(M_L) \gg t_{\text{MS}}(M_{2i})$. Perhaps, the most convenient age can be found by using the mean mass of the secondary components during binary evolution:

$$\overline{M}_2 = \frac{M_{2i} + M_L}{2} \quad (4)$$

Then, we can take $t_{\text{SD}} + t_{\text{CB}}$ as

$$t_{\text{SD}} + t_{\text{CB}} \approx t_{\text{MS}}(\overline{M}_2). \quad (5)$$

If we insert $t_{\text{D}} = t_{\text{MS}}(M_{2i})$ and equation (5) in equation (2), we find the age of an A-subtype CB:

$$t \approx t_{\text{MS}}(M_{2i}) + t_{\text{MS}}(\overline{M}_2). \quad (6)$$

The results of this simple method are listed in Table A1. The basic properties of these binaries are given in Paper I. Although age of a CB is a very complicated problem and may be computed in a variety of ways, the present method gives reasonable results. The average age for the A-subtype CBs is 4.37 Gyr. This value is, surprisingly, in very good agreement with the age found for A-type CBs by Bilir et al. (2005), 4.48 Gyr. The results are listed in Table 1.

In Table A1, uncertainties in ages of CBs are also listed. These uncertainties are derived from equation (6):

$$\Delta t = \frac{\partial t}{\partial M_2} \Delta M_2 + \frac{\partial t}{\partial M_{2i}} \Delta M_{2i}. \quad (7)$$

The uncertainty in ΔM_{2i} as a function of ΔM_2 and ΔL_2 is given in equation 11 of Paper I. The mean uncertainty given in Table 1 is the average of the uncertainties in age of individual binaries listed in Table A1.

3.2 Age of W-subtype CBs

If M_{2i} is less than $1.8 M_{\odot}$, then both components have a convective

tive envelope, and magnetic braking is active in both stars. The angular momentum loss rate of these binaries is nearly twice as fast as the precursors of the A-subtype CBs. Rapid angular momentum evolution causes the secondary component to fill its Roche lobe before it completes its MS lifetime. One should notice that a star of $1.8M_{\odot}$ is an early-type star near the zero-age main-sequence (ZAMS) line and a convective envelope develops as it evolves towards TAMS. The outer convective structure of such a star is very similar to that of a star with $1.5M_{\odot}$ near the ZAMS line. That is to say, stars of $1.8M_{\odot}$ have no role in magnetic braking near ZAMS but are very effective near TAMS. Another reason for the relatively thick convective envelope is high metallicity. These might be the reason for why transition from A- to W-subtype occurs at $M = 1.8M_{\odot}$. The longest detached phase for A-subtype is $t_D = t_{MS}(1.8M_{\odot}) = 1.4$ Gyr. Since the W-subtype CBs have two effective component stars, the typical value of their t_D is $\approx t_{MS}(1.8M_{\odot})/2$. For precursors of typical W-subtype systems, the detached phase lasts about 0.7 Gyr. There are some such very young W UMa-type systems, for example, TX Cnc in Praesepe (see Table 2).

As discussed above, the detached phase of the progenitors of W-subtype CBs takes less time than the MS lifetime of the component stars. This means that component stars touch each other before their massive component reaches the TAMS line. For some systems, the angular momentum evolution is so fast that the detached phase is much shorter than the MS lifetime of the secondary components. In such a case, the massive component is around the ZAMS line. Therefore, equation (2) is not suitable for W-subtypes because the duration of the detached phase might be shorter than the MS lifetime. In this case, the right-hand side of equation (5) can be taken as the age of these systems:

$$t \approx t_{MS}(\overline{M}_2). \quad (8)$$

Equation (8) is valid if detached phase is negligibly small, i.e. $t_D/t \approx 0$. If it is not so small, then we can take, for example, $t_D \approx t_{MS}(M_{2i})/2$ and test which t_D is in better agreement with the observations than the other.

The average ages with negligible and non-negligible t_D are 4.63 and 5.49 Gyr, respectively. The result with $t_D/t \approx 0$ is in very good agreement with the value found by Bilir et al. (2005), 4.37 Gyr. Therefore, the ages of the systems with $t_D/t \approx 0$ are listed in Table A1. The mean uncertainty in the mean age is found as 1.48 Gyr. The mean results are also given in Table 1.

3.3 Comparison of A- and W-subtype of CBs and the cluster member close binaries in period–age diagram

The ages we find for both A- and W-subtypes are in very good agreement with the kinematical ages given by Bilir et al. (2005). We can also compare our findings with the cluster member close binaries in period–age diagram. In Fig. 4, the periods of the A- and the W-subtypes are plotted with respect to their ages, together with the cluster member close binaries compiled by Bukowiecki et al. (2012). The data of Bukowiecki et al. (2012) contain W UMa- and β -Lyrae-type close binaries. It is seen that there is no one-to-one relation between age and period. Any cluster has close binaries with very different periods. The solid line shows the curve fitted by Bukowiecki et al. (2012) for both type close binaries. Although the curve represents a tendency, its uncertainty is very high. The age–period relation of W-subtype has the same tendency as the curve derived by Bukowiecki et al. (2012). For A-subtype, however, the difference is significant for relatively young systems with

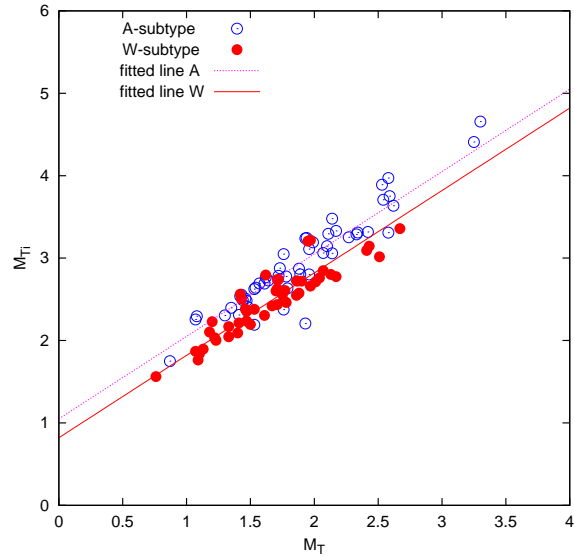


Figure 3. Total initial mass of CBs as a function of total present mass. The fitted curves for A- and W-subtypes are $M_{Ti}/M_{\odot} = M_T/M_{\odot} + (1.05 \pm 0.05)$ and $M_{Ti}/M_{\odot} = M_T/M_{\odot} + (0.82 \pm 0.02)$, respectively.

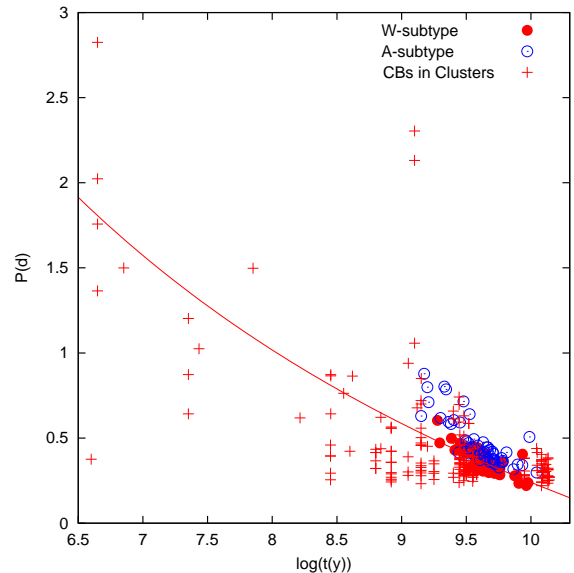


Figure 4. Age–period relation for the A- and W-subtype CBs. The solid line is for the fitted curve derived by Bukowiecki et al. (2012) for W UMa and β Lyrae ($P(d) = 31.19/\log t(y) - 2.87$) type CBs.

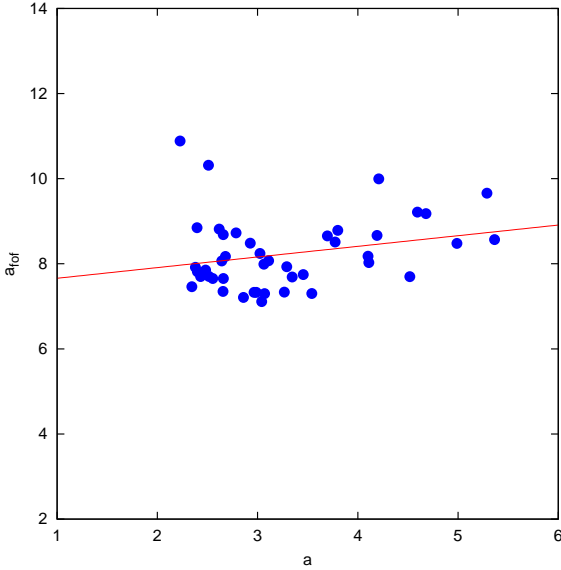
$P > 0.5$ d. The ages of W-subtype CBs from the fitting formula of Bukowiecki et al. (2012) are also listed in Table A1 (t_B). The mean difference between the ages from the fitting formula and from equation (6) or (8) is 36 %.

3.4 Ages of TX Cnc, AH Vir, QX And and AH Cnc, and their clusters

In our W UMa data sample, four binaries are cluster member. The ages of these binaries are given in Table 2. If we compare the ages of binaries with those of clusters, we notice that the cluster age is very low for TX Cnc. This system is perhaps the youngest of the

Table 2. Cluster member CBs.

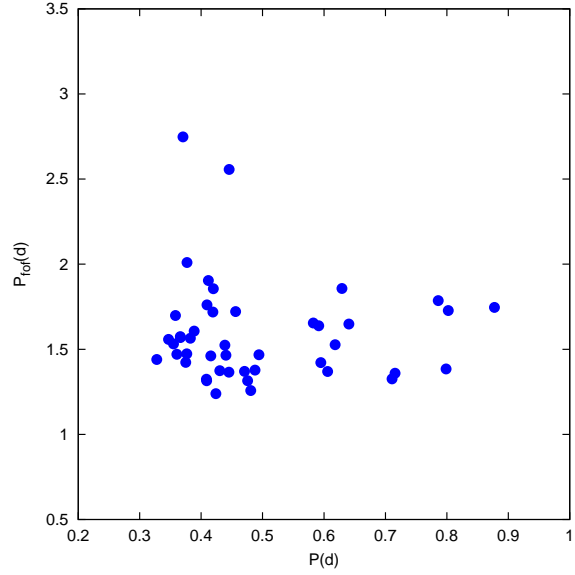
Star	M_{1i}	M_{2i}	$t_{MS}(\text{Gyr})$	$t(\text{Gyr})$	$t_B(\text{Gyr})$	$t_{cl}(\text{Gyr})$	St.	Cluster
TX Cnc	0.50	1.70	1.6	3.90	3.63	0.7	W	Praesepe
AH Vir	0.94	1.67	1.7	3.25	3.08	3.0	W	Wolf 630
QX And	0.62	1.92	1.1	4.29	3.00	2.0	A	NGC 752
AH Cnc	0.93	1.85	1.3	4.81	4.24	4.0	A	M67

**Figure 5.** a_{fof} with respect to a , in units of solar radius. $\overline{a_{\text{fof}}} = 8.1R_{\odot}$. The fitted line is $a_{\text{fof}}/R_{\odot} = (0.25 \pm 0.15)a/R_{\odot} + (7.41 \pm 0.49)$.

whole data set. The age we find for QX And, however, is twice the cluster age. For the other two binary systems, the age differences seem acceptable. For AH Vir, for example, the differences between the three ages are less than 8 per cent. Therefore, it should be stated that our method for age computation is better for A-subtype than for W-subtype. This is in contrast to the result obtained from comparison of our results with the data of the close binaries in clusters (see Section 3.3). The greatest difference appears for the youngest system TX Cnc. Such exceptional binaries must either have very low angular momentum or very high angular momentum loss rate, or both. However, we notice that the difference between the age of the present study and the cluster age depends on M_{1i} : the smaller the value of M_{1i} , the greater is the difference ($t - t_{cl}$).

4 ESTIMATION OF ORBITAL PARAMETERS AT THE FIRST OVERFLOW

For the computation of mean angular momentum and mass-loss rates in CBs, semimajor axis a and P are required at a certain time, in addition to the initial masses of the components. a can be computed from the expression for the effective radius of Roche lobe given by Eggleton (1983). It seems reasonable to assume that, at least for A-subtypes, the mass transfer starts when the massive component of the detached phase fills its Roche lobe the first time. This point is known as the FOF. Then, the Roche lobe radius can be taken as $R_{\text{TAMS}}(M_{2i})$. The distance between the component stars

**Figure 6.** P_{fof} with respect to P , in units of day. $\overline{P_{\text{fof}}} = 1.6$ d.

at FOF is

$$a_{\text{fof}} = \frac{0.6q_i^{-2/3} + \ln(1 + q_i^{-1/3})}{0.49q_i^{-2/3}} R_{\text{TAMS}}. \quad (9)$$

Note that $q_i^{-1} = M_{1i}/M_{2i}$. The values of a_{fof} found from equation (9) are plotted with respect to the present a in Fig. 5. a_{fof} ranges from 7 to 11 R_{\odot} and has a mean value of 8.1 R_{\odot} . There is a weak correlation between a_{fof} and the present a .

Using Kepler's third law

$$P_{\text{fof}} = 0.1159(a_{\text{fof}}^3/(M_{1i} + M_{2i}))^{0.5}, \quad (10)$$

the period (P_{fof}) at the end of the pre-contact phase is available. P_{fof} given in equation (10) is in units of days and plotted with respect to the present period P in Fig. 6. P_{fof} ranges from 1.24 to 2 d, except two A-subtype systems. The mean value of P_{fof} is about 1.6 d. Although there is no correlation between P_{fof} and P confirmed for the full range, there is an inverse relation for small values of P ($0.5 < P$).

P_{fof} and a_{fof} are given in Table A1. For W-subtypes, the values should be considered as just upper limits.

4.1 Angular momentum evolution of W UMa-type CBs.

Assuming components as point masses, the orbital angular momentum of a binary is given by

$$J = 1.24 \times 10^{52} (M_1 + M_2)^{5/3} P^{1/3} \frac{q}{(1+q)^2} \text{ g cm}^{-2} \text{ s}^{-1} \quad (11)$$

where masses are in units of solar masses and P in units of day. The angular momentum at the time of the FOF (J_{fof}) can be computed from equation (11) by using initial masses, and P_{fof} . $\log(J_{\text{fof}})$ is plotted with respect to the present angular momentum $\log(J)$ in Fig. 7. There is a power-law relation between J_{fof} and J . The solid line is the fitting line. The slope in Fig. 7 is 0.46, which implies that $J_{\text{fof}} \propto J^{0.46}$. That is to say, the present angular momentum depends on angular momentum at the time of the FOF:

$$J \propto J_{\text{fof}}^{2.2}. \quad (12)$$

For systems with the lowest angular momentum, $\Delta \log(J) =$

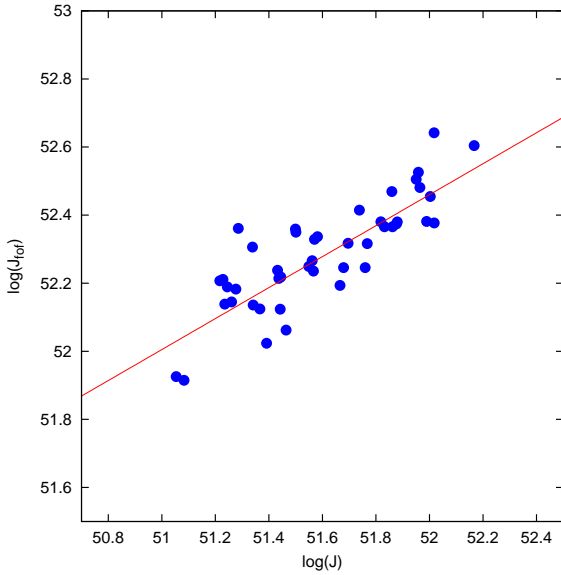


Figure 7. $\log(J_{\text{fof}})$ with respect to $\log(J)$, in cgs units. The fitted line is $(0.46 \pm 0.05) \log(J) + (28.8 \pm 1.4)$

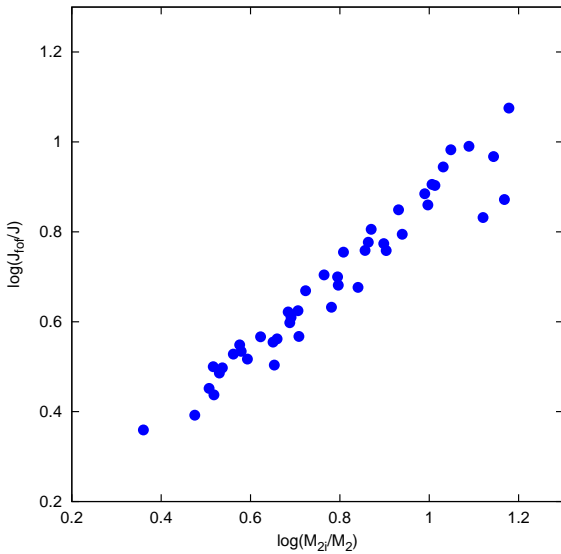


Figure 8. Logarithmic change in angular momentum with respect to that of the secondary mass.

$\log(J_{\text{fof}}/J) \approx 1.0$. This means that the present angular momentum of these systems is one tenth of J_{fof} . For systems with the highest angular momentum, however, $\Delta \log(J) = \log(J_{\text{fof}}/J) \approx 0.4$. In this case, the present angular momentum is two fifths of J_{fof} . In Fig. 8, logarithmic change in angular momentum is plotted with respect to logarithmic change in mass of the secondaries. It seems that the present mass of the secondary stars is determined by the amount of angular momentum loss after FOF.

4.2 Angular momentum evolution in the contact phase

Angular momentum loss rate in any phase of a binary system depends on its mass-loss rate and angular momentum content. In Fig. 9, angular momentum of A-subtype CBs at different evolutionary

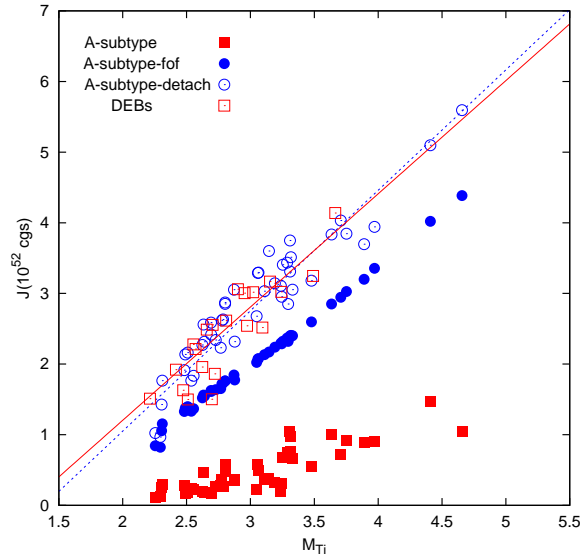


Figure 9. Angular momentum with respect to initial mass for A-subtype W UMa-type CBs through their past evolutionary phases from detached to contact. The squares are for the well-known eclipsing binaries (DEBs) having the same mass range as the initial masses of W UMa-type CBs. The solid and dotted lines are for the fitted lines for DEBs and the estimated initial angular momentum of A-subtype CBs in the detached phase, respectively.

phases is plotted with respect to the total initial mass (M_{Ti}). The A-subtype CBs have lost a large part of their angular momentum and therefore take place in the lower part of Fig. 9. In Fig. 9, their angular momentum at the time of the FOF (J_{fof}) is also plotted. On average, these binaries have lost 78 per cent of their J_{fof} (the range 55–90 per cent) during the SD and contact phases; the larger the angular momentum is, the higher is the loss rate. Following several attempts, we derive a fitting formula for the angular momentum after FOF as a function of initial masses:

$$\frac{dJ}{dt} = -3.71 \times 10^{41} M_{1i}^{0.82} M_{2i}^4 \text{ g cm}^{-2} \text{ s}^{-1} \text{ y}^{-1}, \quad (13)$$

where masses are in solar masses. Similarly, we derive another fitting formula for mass-loss:

$$\frac{dM}{dt} = -2.0 \times 10^{-11} M_{2i}^{4.38} M_{\odot} \text{ y}^{-1} \quad (14)$$

The angular momentum and mass-loss rates are plotted with respect to M_{2i} in Fig. 10. We note that these two formulae are very strong functions of M_{2i} as luminosity. This may imply that nuclear evolution of M_{2i} dominates orbital evolution mainly driven by M_{1i} .

Our present consideration does not allow for consideration of the SD and CB phases separately. The angular momentum and mass-losses should be estimated in order to ascertain the final product of W UMa-type CBs. A study of near-CBs could help with this.

4.3 Angular momentum evolution in the detached phase

We compute typical angular momentum (J_0) in order to assess angular momentum evolution of precursors of A-subtype CBs in the detached phase. The angular momentum is a function of the total mass M_{Ti} in all phases. Angular momentum loss in the detached phase, however, depends on the convective structure of the primary components with a mass of M_{1i} . Therefore, we assume that the loss

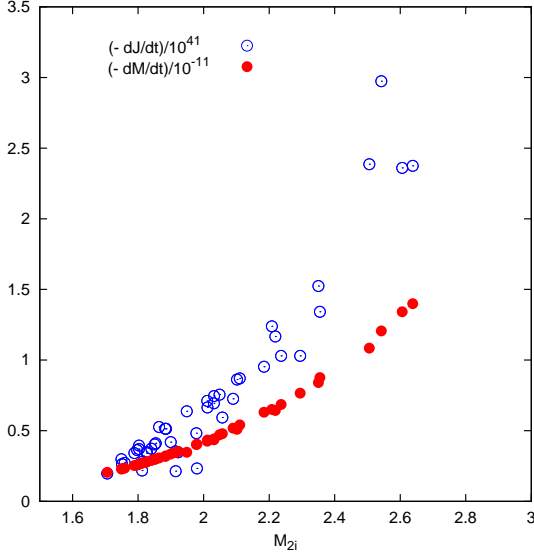


Figure 10. Angular momentum (circle) and mass-loss (filled circle) rates with respect to initial mass of the secondaries. The units of angular momentum and mass-loss rates are $\text{g cm}^{-2}\text{s}^{-1}\text{y}^{-1}$ and $M_{\odot}\text{y}^{-1}$, respectively. Note that dJ/dt and dM/dt are multiplied by -1 .

rate (dJ/dt) is a function of M_{1i} :

$$\frac{dJ}{dt} = -c_J M_{1i}^n, \quad (15)$$

where c_J and n are free parameters to be determined from fitting J_0 to the angular momentum of the well-known DEBs (J_{DEB}),

$$J_{\text{fof}} = J_0 + \frac{dJ}{dt} \delta t = J_0 + \frac{dJ}{dt} t_{\text{MS}}. \quad (16)$$

Then, we find the expression for J_0 in terms of J_{fof} and M_{1i} :

$$J_0 = J_{\text{fof}} - c_J M_{1i}^n t_{\text{MS}}. \quad (17)$$

The unit of c_J is the same as the angular momentum. If we take M_{1i} and t_{MS} in units of solar mass and in units of year, respectively, we find the value of c_J and n by fitting J_0 to the angular momentum of DEBs as $c = 0.8 \times 10^{43}$ (cgs) and $n = 1.5$:

$$\frac{dJ}{dt} = 0.8 \times 10^{43} M_{1i}^{1.5}. \quad (18)$$

The dotted and solid lines in Fig. 9 represent the fitting lines for the DEBs and detached progenitors of W UMa binaries, respectively. They are very close to each other. The progenitors of A-subtype CBs have lost 13–40 per cent of their initial angular momentum during the detached phase, with a mean value of 29 per cent. However, most of their angular momentum is lost during the SD and CB phases. The total angular momentum lost by the progenitors of the A-subtype CBs' overall phases is about 84 per cent, i.e. the initial angular momentum of these binaries was six to seven times greater than their present angular momentum.

The mean values of a_0 and P_0 are found from J_0 given in equation (17) as $16.3 R_{\odot}$ and 4.5 d, respectively. While a_0 ranges from 13.3 to $19.7 R_{\odot}$, the interval for P_0 is from 2.8 to 6.3 d. a_0 and P_0 are given in Table A1.

4.4 Comparison of angular momentum loss rates in the detached phase

It is well known that the angular momentum loss rate for early-type stars is very slow in comparison with late-type stars. Therefore, the rate we derive for the detached phase of A-subtype CBs is only a function of the mass of their late-type component (M_{1i}). Stępień (2006) gives the rate for close binaries as (see also Gazeas & Stępień 2008)

$$\frac{dJ}{dt} = -4.9 \times 10^{41} (R_1^2 M_1 + R_2^2 M_2) / P, \quad (19)$$

where masses and radii are in solar units, period is in days, time in years and angular momentum in cgs units. Equation (19) is a semi-empirical formula based on the angular momentum rate of single late-type stars. The expression we derive is much easier than that of Stępień (2006). The mean ratio of the rate given in equation (18) to that of equation (19) for the detached phase is 0.63, which is satisfactory agreement. If we compute the initial angular momentum by going back from FOF, the initial angular momentum difference between the two rates is about 10 per cent.

Demircan et al. (2006) derive the time variation of angular momentum for detached chromospherically active binaries (CABs) as

$$J = J_0 e^{-3.48 \times 10^{-10} t}. \quad (20)$$

We also compare our results with that given by equation (20). The mean ratio of the rate given in equation (18) to that of equation (20) is 0.77 for the detached phase. Many of the CABs studied by Demircan et al. are not in the initial mass range of W UMa-type CBs. Despite this fact, the agreement between the two rates is very impressive. The rate given in equation (18) is found from fitting the initial angular momentum of A-subtype to that of the well-known detached binaries with a period less than 5 d. In order to obtain better agreement between this rate and that of Demircan et al. (2006), the upper limit for the period should be reduced to 4.45 d. Then, $c_J = 0.6 \times 10^{43}$ (cgs) for this upper limit. This may imply that, in addition to the constraints on the initial masses of the components, the detached binaries with $P < 4.45$ d become A-subtype CBs.

5 CONCLUSIONS

In Paper I, a new method is developed for estimating initial masses of component stars in W UMa-type CBs, based on introducing mass according to the luminosity of the secondaries. In the present study, it is shown that an additional clue is the $M_L - R_2$ relation for secondary stars to support the idea that the structure and evolution of these stars primarily depend on M_L : $M_L - R$ relation being in good agreement with that of normal stars of detached binaries.

Using the initial mass and mass according to luminosity, a new method is developed for age estimation of A- and W-subtypes. This is the first time that such a method of age estimation for W UMa-type CBs has been derived from the fundamental properties of secondary components. We apply this method and find that the mean ages of A- and W-subtypes are 4.4 and 4.6 Gyr, respectively. These values are in very good agreement with the kinematic ages found by Bilir et al. (2005). The ages we find are also compared with the ages of cluster member close binaries. The agreement is satisfactory for stellar age, provided that the binary is not very young.

Our data sample contains four cluster member W UMa-type CBs; two A- and two W-subtypes. The ages we find are in good

agreement with the cluster ages, if M_{1i} is about $1 M_{\odot}$. The difference is great for the CBs with $M_{1i} \approx 0.5-0.6 M_{\odot}$. Determination of stellar parameters of such cluster member binaries is very important for our understanding of binary evolution.

We show that there is a strong correlation between the present mass of primary (M_1) and the total initial mass (M_{Ti}). If we estimate (M_1) from this, the difference between the observed and the estimated values of M_1 is very small, being less than 10 per cent. This implies that M_1 either remains constant or changes very little during the W UMa phase, if at all.

The discovery of initial masses of W UMa-type CBs in terms of observed quantities leads us to consider the binary evolution of these systems. We compute the properties of A-subtype CBs at the time of the FOF by using Eggleton's (1983) expression for the effective radius of Roche lobe. The mean distance between the component stars in the former case is about $\overline{a_{fof}} = 8 R_{\odot}$ and the mean period is $\overline{P_{fof}} = 1.6$ d. Computation of the period or mean distance enables us to also consider the angular momentum evolution of these systems. We find that angular momentum at FOF is 2.5–10 times greater than the present angular momentum. That is to say, these systems have lost a great deal of their angular momentum during the contact phase (SD+CB).

For estimation of initial angular momentum in the detached phase, we compare J_{fof} with the angular momentum of the well-known DEBs. Satisfactory agreement is obtained if the rate of angular momentum loss in the detached phase is directly proportional to $M_{1i}^{1.5}$. The rate we derive is in very good agreement with the rates of Stępień (2006) and Demircan et al. (2006). We find that $\overline{a_0} = 16.3 R_{\odot}$ and $\overline{P_0} = 4.5$ d. In addition to the initial mass intervals for the components of W UMa-type CBs, we also obtain an upper limit for the initial period.

ACKNOWLEDGEMENT

I would like to thank Ros Elliot for her help in checking the language of the manuscript.

REFERENCES

- Bilir S., Karataş Y., Demircan O., Eker Z., 2005, MNRAS, 357, 497
 Bukowiecki L., Maciejewski G., Konorski P., Errmann R., 2012, Inf. Bull. Var. Stars, 6021, 1
 Demircan O., Eker Z., Karataş Y., Bilir S., 2006, MNRAS, 366, 1511
 Eggleton P.P., 1983, ApJ, 268, 368
 Eggleton P.P., 2001, in Podsiadlowski Ph., Rappaport S., King A.R., D'Antona F., Burder L., eds, ASP Conf. Ser. Vol.229, Evolution of Binary and Multiple Star Systems, Astron. Soc. Pac., San Francisco, p. 157
 Eker Z., Demircan O., Bilir S., 2008, MNRAS, 386, 1756
 Gazeas K., Stępień K., 2008, MNRAS, 390, 1577
 Hilditch R.W., King D.J., McFarlane T.M., 1988, MNRAS, 231, 341
 Li L., Zhang F., Han Z., Jiang D., 2007, ApJ, 662, 596
 Miglio A., Montalbán J., 2005, A&A, 441, 615
 Paxton B., Bildsten L., Dotter A., Herwig F., Lesaffre P., Timmes F., 2011, ApJS, 192, 3
 Stępień K., 2006, Acta Astron., 56, 347

- Tutukov A.V., Dremova G.N., Svechnikov M.A., 2004, Astron. Rep., 48, 219
 van 't Veer F., 1991, A&A, 250,84
 Yıldız M., 2007, MNRAS, 374, 1264
 Yıldız M., 2013, submitted
 Yıldız M., Doğan T., 2013, MNRAS, 430, 2029

APPENDIX A: BASIC PROPERTIES OF W UMA TYPE BINARIES

Table A1: Initial and present properties of the A- and W-subtype CBs. The columns are organized as name, subtype, semimajor axis, period, primary and secondary masses, initial masses of primary and secondary before the mass transfer, mass of secondary according to luminosity, age (see Section 3), age from Bukowiecki et al. (2012), semimajor axis and period at FOF, and initial semimajor axis and period.

Star	Type	a (R_{\odot})	P (d)	M_1 (M_{\odot})	M_2 (M_{\odot})	$M_{1,i}$ (M_{\odot})	$M_{2,i}$ (M_{\odot})	M_L (M_{\odot})	t (Gyr)	t_B (Gyr)	a_{fof} (R_{\odot})	P_{fof} (d)	a_D (R_{\odot})	P_D (d)
HV UMa	A	4.988	0.711	2.80±0.60	0.50±0.17	2.11±0.57	2.54±0.69	1.30±0.12	1.62±1.89	0.48	8.48	1.33	13.80	2.75
V376 And	A	5.364	0.799	2.49±0.06	0.76±0.03	1.90±0.10	2.51±0.13	1.40±0.02	1.58±0.35	0.30	8.57	1.38	13.77	2.82
RR Cen	A	4.110	0.606	2.09±0.43	0.45±0.10	1.50±0.25	2.21±0.38	1.10±0.04	2.53±1.77	0.89	8.03	1.37	15.04	3.51
V921 Her	A	5.288	0.877	2.07±0.05	0.51±0.03	1.37±0.05	2.61±0.09	1.34±0.00	1.50±0.20	0.20	9.66	1.75	13.32	2.83
UZ Leo	A	4.192	0.618	1.99±0.04	0.60±0.02	1.40±0.04	2.35±0.07	1.24±0.01	2.00±0.24	0.82	8.67	1.53	13.99	3.13
V535 Ara	A	4.209	0.629	1.94±0.04	0.59±0.02	1.25±0.07	2.64±0.15	1.39±0.06	1.41±0.39	0.77	10.00	1.86	13.34	2.86
AQ Tuc	A	4.102	0.595	1.93±0.21	0.69±0.08	1.42±0.20	2.22±0.32	1.22±0.03	2.31±1.33	0.95	8.18	1.42	14.80	3.46
EF Dra	A	3.041	0.424	1.81±0.00	0.29±0.00	1.28±0.00	1.86±0.00	0.84±0.00	4.63±0.00	2.76	7.11	1.24	19.56	5.66
V2388 Oph	A	4.681	0.802	1.80±0.02	0.34±0.01	1.12±0.02	2.35±0.04	1.12±0.01	2.14±0.16	0.29	9.18	1.73	13.77	3.17
AW UMa	A	3.024	0.439	1.79±0.14	0.14±0.01	1.13±0.02	2.11±0.03	0.90±0.00	3.26±0.17	2.51	8.24	1.52	15.10	3.78
V776 Cas	A	3.063	0.440	1.75±0.04	0.24±0.02	1.14±0.05	2.05±0.08	0.91±0.01	3.47±0.59	2.48	7.99	1.47	15.74	4.05
V592 Per	A	4.519	0.716	1.74±0.06	0.68±0.04	1.29±0.10	2.03±0.15	1.13±0.01	3.01±0.88	0.47	7.70	1.36	16.41	4.23
XZ Leo	A	3.456	0.488	1.74±0.05	0.59±0.03	1.26±0.06	2.03±0.10	1.08±0.00	3.11±0.59	1.83	7.75	1.38	16.30	4.21
DK Cyg	A	3.345	0.471	1.74±0.00	0.53±0.00	1.24±0.00	2.01±0.00	1.04±0.00	3.29±0.00	2.04	7.69	1.37	16.54	4.32
NN Vir	A	3.540	0.481	1.73±0.02	0.85±0.02	1.36±0.06	1.95±0.08	1.20±0.01	3.18±0.53	1.91	7.30	1.26	18.09	4.90
η CrA	A	3.697	0.591	1.72±0.04	0.22±0.02	1.06±0.03	2.18±0.06	0.98±0.00	2.83±0.28	0.97	8.66	1.64	14.44	3.53
RZ Tau	A	3.111	0.416	1.70±0.16	0.64±0.06	1.21±0.14	2.10±0.25	1.14±0.03	2.76±1.33	2.92	8.07	1.46	15.37	3.84
V401 Cyg	A	3.800	0.583	1.68±0.00	0.49±0.00	1.09±0.00	2.24±0.00	1.13±0.00	2.40±0.00	1.02	8.79	1.65	14.20	3.40
AQ Psc	A	3.267	0.476	1.68±0.03	0.39±0.02	1.18±0.04	1.89±0.07	0.91±0.00	4.27±0.59	1.98	7.33	1.32	18.45	5.25
AH Aur	A	3.290	0.494	1.68±0.05	0.28±0.01	1.10±0.02	2.01±0.04	0.91±0.01	3.63±0.31	1.76	7.93	1.47	16.03	4.22
V839 Oph	A	2.987	0.409	1.64±0.00	0.50±0.00	1.18±0.00	1.88±0.00	0.97±0.00	4.08±0.00	3.05	7.33	1.32	18.49	5.27
FP Boo	A	3.774	0.640	1.61±0.05	0.15±0.02	0.96±0.03	2.09±0.06	0.89±0.00	3.36±0.39	0.72	8.51	1.65	14.90	3.82
V1073 Cyg	A	4.595	0.786	1.60±0.02	0.51±0.01	1.00±0.01	2.29±0.03	1.17±0.00	2.21±0.13	0.32	9.21	1.79	13.90	3.31
EX Leo	A	2.859	0.409	1.57±0.03	0.31±0.02	1.07±0.05	1.80±0.08	0.83±0.01	5.12±0.93	3.06	7.21	1.32	19.72	5.99
AP Leo	A	2.965	0.430	1.46±0.04	0.43±0.02	1.00±0.06	1.80±0.11	0.89±0.02	4.83±1.18	2.65	7.33	1.37	19.23	5.84
FG Hya	A	2.344	0.328	1.45±0.03	0.16±0.01	0.90±0.02	1.79±0.04	0.74±0.00	5.66±0.50	5.31	7.46	1.44	18.89	5.80
UX Eri	A	3.070	0.445	1.43±0.03	0.53±0.02	1.00±0.05	1.80±0.10	0.94±0.01	4.65±1.02	2.40	7.30	1.37	19.41	5.92
YY CrB	A	2.659	0.377	1.43±0.03	0.35±0.01	0.93±0.02	1.85±0.05	0.87±0.01	4.61±0.46	3.80	7.65	1.47	17.73	5.19
CK Boo	A	2.452	0.355	1.42±0.00	0.15±0.00	0.85±0.00	1.84±0.00	0.76±0.00	5.16±0.00	4.40	7.78	1.53	17.51	5.17
V566 Oph	A	2.785	0.410	1.40±0.03	0.33±0.01	0.82±0.01	2.06±0.03	0.96±0.00	3.31±0.21	3.04	8.72	1.76	14.87	3.92
TYC1174 a	A	2.642	0.389	1.38±0.01	0.26±0.01	0.83±0.02	1.90±0.04	0.85±0.01	4.41±0.39	3.50	8.07	1.61	16.47	4.69
CN Hyi	A	2.927	0.456	1.37±0.06	0.25±0.02	0.79±0.07	1.98±0.16	0.88±0.05	3.88±1.48	2.24	8.48	1.72	15.45	4.23
GR Vir	A	2.399	0.347	1.37±0.16	0.17±0.06	0.81±0.10	1.83±0.23	0.76±0.02	5.25±2.63	4.65	7.81	1.56	17.54	5.24
DZ Psc	A	2.481	0.366	1.35±0.06	0.18±0.02	0.80±0.03	1.83±0.08	0.77±0.01	5.22±0.87	4.08	7.85	1.57	17.45	5.22
HN Uma	A	2.515	0.383	1.28±0.06	0.18±0.01	0.75±0.02	1.76±0.06	0.74±0.01	5.93±0.83	3.65	7.70	1.56	18.46	5.80
V410 Aur	A	2.432	0.366	1.27±0.06	0.17±0.03	0.74±0.05	1.75±0.11	0.73±0.01	6.06±1.52	4.07	7.70	1.57	18.56	5.87
SX Crv	A	2.160	0.317	1.25±0.04	0.10±0.01	0.72±0.02	1.68±0.05	0.66±0.01	7.32±0.97	5.75	7.44	1.52	20.33	6.86
EQ Tau	A	2.481	0.341	1.22±0.03	0.54±0.02	0.91±0.06	1.47±0.09	0.82±0.01	8.56±2.04	4.84	6.24	1.17	35.53	15.92
Y Sex	A	2.657	0.420	1.21±0.15	0.22±0.03	0.64±0.05	1.91±0.15	0.83±0.03	4.38±1.44	2.84	8.68	1.86	15.62	4.48
V2357 Oph	A	2.670	0.416	1.19±0.01	0.29±0.01	0.72±0.02	1.68±0.04	0.76±0.00	6.47±0.62	2.92	7.47	1.53	20.10	6.74
V404 Peg	A	2.679	0.419	1.18±0.00	0.29±0.00	0.67±0.00	1.82±0.00	0.82±0.00	5.06±0.00	2.85	8.17	1.72	16.93	5.12
QX And	A	2.617	0.412	1.18±0.17	0.24±0.04	0.61±0.05	1.92±0.17	0.85±0.03	4.29±1.58	3.00	8.81	1.90	15.48	4.43
VZ Lib	A	2.380	0.358	1.06±0.06	0.35±0.03	0.60±0.05	1.71±0.13	0.80±0.02	6.00±1.89	4.30	7.92	1.70	18.51	6.07
OO Aql	A	3.329	0.507	1.05±0.02	0.88±0.02	0.91±0.23	1.30±0.33	1.01±0.05	9.75±9.25	1.62	5.61	1.04	64.99	40.89
V508 Oph	A	2.383	0.345	1.01±0.00	0.52±0.00	0.68±0.00	1.51±0.00	0.83±0.00	7.90±0.00	4.72	6.91	1.42	26.47	10.67
DX Tuc	A	2.396	0.377	1.00±0.03	0.30±0.01	0.49±0.02	1.81±0.06	0.82±0.01	5.06±0.67	3.78	8.85	2.01	16.16	4.96
TV Mus	A	2.510	0.446	0.94±0.14	0.13±0.02	0.34±0.02	1.91±0.12	0.79±0.03	4.55±1.34	2.40	10.31	2.56	15.20	4.58
XY Boo	A	2.227	0.371	0.93±0.34	0.15±0.05	0.32±0.02	1.98±0.15	0.83±0.00	4.03±1.13	3.96	10.89	2.75	15.07	4.48
TZ Boo	A	1.790	0.298	0.72±0.05	0.15±0.04	0.28±0.04	1.47±0.19	0.59±0.03	11.05±5.80	6.58	8.57	2.20	20.56	8.17
AH Cnc	A	2.553	0.360	1.47±0.15	0.25±0.03	0.93±0.08	1.85±0.16	0.82±0.03	4.81±1.78	4.24	7.65	1.47	17.70	5.17
RT LMi	A	2.656	0.375	1.31±0.05	0.48±0.03	0.88±0.07	1.75±0.13	0.90±0.01	5.18±1.54	3.84	7.35	1.42	19.74	6.27
DN Cam	W	3.668	0.498	1.85±0.02	0.82±0.02	1.50±0.07	1.86±0.09	1.15±0.01	1.26±0.37	1.71	6.82	1.13	13.81	3.25
V728 Her	W	3.183	0.471	1.65±0.00	0.30±0.00	1.01±0.00	2.19±0.00	1.02±0.00	1.80±0.00	2.03	8.78	1.68	13.80	3.32
V402 Aur	W	3.766	0.604	1.64±0.05	0.33±0.02	1.01±0.03	2.21±0.08	1.04±0.01	1.84±0.25	0.90	8.86	1.70	13.85	3.33
EF Boo	W	3.220	0.430	1.61±0.00	0.82±0.00	1.25±0.00	1.90±0.00	1.05±0.00	1.95±0.00	2.66	7.27	1.28	13.33	3.18
ET Leo	W	2.670	0.347	1.59±0.02	0.54±0.01	1.25±0.05	1.55±0.05	0.79±0.00	2.03±0.58	4.67	6.07	1.03	12.71	3.14
AA UMa	W	3.400	0.468	1.56±0.00	0.85±0.00	1.21±0.00	1.88±0.00	0.99±0.00	2.15±0.00	2.07	7.26	1.29	13.22	3.17
YY Eri	W	2.553	0.321	1.55±0.14	0.62±0.07	1.24±0.53	1.53±0.45	0.78±0.03	2.20±5.57	5.57	6.01	1.02	12.66	3.13

Table A1: – continued from previous page

Star	Type	a (R_{\odot})	P (d)	M_1 (M_{\odot})	M_2 (M_{\odot})	M_{1i} (M_{\odot})	M_{2i} (M_{\odot})	M_L (M_{\odot})	t (Gyr)	t_B (Gyr)	a_{tof} (R_{\odot})	P_{tof} (d)	a_D (R_{\odot})	P_D (d)
ER Ori	W	3.224	0.423	1.53±0.00	0.98±0.00	1.27±0.00	1.74±0.00	1.05±0.00	2.29±0.00	2.77	6.70	1.16	13.07	3.15
V502 Oph	W	3.162	0.453	1.51±0.28	0.56±0.08	1.12±0.23	1.73±0.36	0.93±0.04	2.39±2.57	2.29	6.88	1.24	12.69	3.10
V870 Ara	W	2.681	0.400	1.50±0.01	0.12±0.01	0.91±0.02	1.89±0.04	0.77±0.00	2.44±0.26	3.25	7.85	1.52	12.75	3.15
BB Peg	W	2.676	0.362	1.42±0.02	0.55±0.01	1.07±0.03	1.59±0.04	0.87±0.00	2.91±0.42	4.21	6.43	1.16	12.29	3.06
VY Sex	W	3.014	0.443	1.42±0.02	0.45±0.01	0.99±0.02	1.73±0.04	0.87±0.00	2.91±0.30	2.43	7.09	1.33	12.44	3.08
V417 Aql	W	2.687	0.370	1.40±0.00	0.50±0.00	0.98±0.00	1.74±0.00	0.90±0.00	3.05±0.00	3.96	7.11	1.33	12.44	3.08
AE Phe	W	2.698	0.362	1.38±0.06	0.63±0.02	1.02±0.14	1.69±0.18	0.87±0.03	3.20±1.62	4.18	6.86	1.26	12.39	3.07
EZ Hya	W	2.958	0.450	1.37±0.00	0.35±0.00	0.85±0.00	1.89±0.00	0.89±0.00	3.14±0.00	2.34	7.96	1.57	12.68	3.16
AH Vir	W	2.797	0.407	1.36±0.00	0.41±0.00	0.94±0.00	1.67±0.00	0.82±0.00	3.35±0.00	3.08	6.95	1.31	12.18	3.05
V842 Her	W	2.817	0.419	1.36±0.00	0.35±0.00	0.84±0.00	1.90±0.00	0.89±0.00	3.08±0.00	2.86	8.04	1.60	12.70	3.17
UV Lyn	W	2.878	0.415	1.36±0.02	0.50±0.01	0.92±0.02	1.80±0.05	0.93±0.01	3.32±0.32	2.93	7.47	1.43	12.51	3.11
W UMa	W	2.568	0.334	1.35±0.09	0.69±0.05	0.99±0.24	1.77±0.32	0.91±0.04	3.44±2.23	5.09	7.24	1.36	12.54	3.10
QW Gem	W	2.557	0.358	1.31±0.04	0.44±0.01	0.90±0.03	1.66±0.06	0.83±0.01	3.79±0.64	4.31	6.97	1.33	12.08	3.04
SS Ari	W	2.758	0.406	1.31±0.00	0.40±0.00	0.84±0.00	1.78±0.00	0.87±0.00	3.65±0.00	3.11	7.57	1.49	12.35	3.10
V752 Cen	W	2.588	0.370	1.30±0.00	0.40±0.00	0.84±0.00	1.76±0.00	0.85±0.00	3.84±0.00	3.97	7.47	1.47	12.27	3.09
AM Leo	W	2.656	0.366	1.29±0.01	0.59±0.01	0.94±0.03	1.64±0.04	0.90±0.00	3.99±0.36	4.09	6.82	1.29	12.10	3.04
V781 Tau	W	2.844	0.408	1.29±0.07	0.57±0.03	0.94±0.08	1.61±0.13	0.89±0.01	3.99±1.19	3.08	6.70	1.26	12.03	3.03
V1191 Cyg	W	2.182	0.313	1.29±0.08	0.13±0.01	0.71±0.01	1.85±0.03	0.76±0.00	3.85±0.21	5.88	8.19	1.70	12.44	3.18
RZ Com	W	2.476	0.339	1.23±0.09	0.55±0.04	0.89±0.12	1.58±0.23	0.89±0.03	4.61±2.34	4.93	6.68	1.28	11.84	3.01
GM Dra	W	2.303	0.339	1.21±0.04	0.22±0.02	0.67±0.02	1.83±0.07	0.79±0.00	3.76±0.49	4.92	8.25	1.74	12.36	3.19
FU Dra	W	2.170	0.307	1.17±0.04	0.29±0.01	0.70±0.02	1.68±0.05	0.76±0.01	4.81±0.51	6.17	7.51	1.55	11.86	3.07
U Peg	W	2.520	0.375	1.15±0.01	0.38±0.01	0.72±0.02	1.66±0.05	0.80±0.01	4.70±0.50	3.84	7.37	1.50	11.81	3.05
AO Cam	W	2.354	0.330	1.12±0.01	0.49±0.01	0.77±0.02	1.54±0.05	0.80±0.00	5.56±0.55	5.24	6.77	1.34	11.51	2.98
GZ And	W	2.279	0.305	1.12±0.02	0.59±0.02	0.75±0.06	1.68±0.10	0.84±0.01	4.27±0.91	6.24	7.39	1.49	11.93	3.06
TW Cet	W	2.320	0.317	1.06±0.00	0.61±0.00	0.68±0.00	1.74±0.00	0.78±0.00	4.32±0.00	5.74	7.82	1.63	12.04	3.11
BV Dra	W	2.376	0.350	1.04±0.02	0.43±0.01	0.59±0.02	1.76±0.05	0.87±0.01	3.72±0.43	4.55	8.21	1.78	12.09	3.17
BX Peg	W	2.016	0.280	1.02±0.12	0.38±0.05	0.67±0.10	1.42±0.20	0.69±0.01	7.76±3.46	7.44	6.55	1.34	11.02	2.93
OU Ser	W	1.989	0.297	1.02±0.01	0.18±0.01	0.50±0.02	1.73±0.05	0.72±0.01	4.72±0.60	6.62	8.44	1.90	11.98	3.22
AB And	W	2.308	0.332	1.01±0.02	0.49±0.01	0.66±0.06	1.54±0.14	0.80±0.04	5.53±2.00	5.16	7.05	1.46	11.35	2.99
SW Lac	W	2.380	0.321	0.98±0.00	0.78±0.00	0.61±0.00	1.88±0.00	0.86±0.00	3.28±0.00	5.59	8.62	1.86	12.51	3.25
TY Boo	W	2.151	0.317	0.93±0.02	0.40±0.01	0.51±0.03	1.66±0.10	0.81±0.03	4.58±1.12	5.73	8.11	1.82	11.71	3.15
VW Cep	W	1.972	0.278	0.93±0.02	0.40±0.01	0.57±0.05	1.48±0.11	0.66±0.02	7.48±2.18	7.56	7.07	1.52	11.05	2.98
BW Dra	W	1.957	0.292	0.92±0.02	0.26±0.01	0.45±0.01	1.65±0.05	0.73±0.01	5.23±0.59	6.84	8.29	1.91	11.69	3.20
TX Cnc	W	2.488	0.383	0.91±0.10	0.50±0.06	0.50±0.08	1.71±0.29	0.89±0.03	3.90±2.32	3.63	8.32	1.87	11.90	3.20
V757 Cen	W	2.345	0.343	0.88±0.00	0.59±0.00	0.49±0.00	1.74±0.00	0.85±0.00	3.94±0.00	4.77	8.53	1.93	12.04	3.24
V829 Her	W	2.273	0.358	0.86±0.02	0.37±0.01	0.47±0.02	1.53±0.05	0.74±0.01	6.09±0.77	4.31	7.68	1.74	11.21	3.07
CC Com	W	1.587	0.221	0.72±0.02	0.38±0.01	0.35±0.07	1.49±0.11	0.53±0.01	9.22±2.53	11.52	8.11	1.97	11.14	3.18
XY Leo	W	1.943	0.284	0.76±0.15	0.46±0.06	0.35±0.26	1.68±0.46	0.63±0.05	5.75±6.06	7.25	9.07	2.22	12.03	3.39
V523 Cas	W	1.662	0.234	0.75±0.03	0.38±0.02	0.36±0.07	1.53±0.13	0.56±0.01	8.06±2.47	10.48	8.23	1.99	11.31	3.20
BH Cas	W	2.373	0.406	0.74±0.06	0.35±0.03	0.40±0.03	1.36±0.12	0.69±0.01	8.61±2.46	3.12	7.23	1.70	10.56	3.00
RW Dor	W	1.866	0.285	0.64±0.00	0.43±0.00	0.24±0.00	1.63±0.00	0.68±0.00	5.71±0.00	7.17	9.84	2.62	12.30	3.66
RW Com	W	1.471	0.237	0.56±0.06	0.20±0.03	0.15±0.01	1.41±0.12	0.59±0.01	9.49±2.80	10.20	9.68	2.79	11.77	3.74

a) TYC 1174-344-1